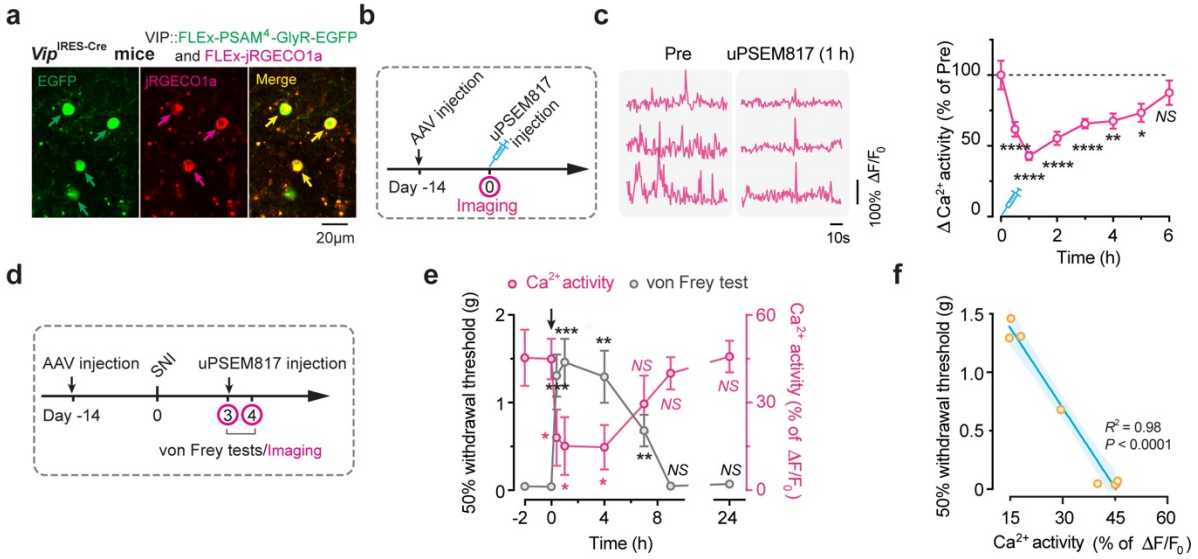

Supplementary Fig. 1 | Intraperitoneal injection of uPSEM817 transiently suppresses VIP neuron activity. **a**, Co-expression of inhibitory chemogenetic module PSAM^4-GlyR and genetically encoded Ca^{2+} indicator jRGECO1a in VIP INs through cortical injection of AAV viruses into the S1 of *Vip*$^{IRES-Cre}$ mice. Green, magenta, and yellow arrows indicate VIP INs expressing PSAM^4-GlyR-EGFP, jRGECO1a, and both, respectively. **b**, Timeline (for **c**) to examine the acute effects of PSAM^4-GlyR activation on VIP IN activity. **c**, Left, representative Ca^{2+} traces of VIP INs expressing PSAM^4-GlyR-EGFP and jRGECO1 before and 1 h after i.p. injection of uPSEM817 (ligand for PSAM^4-GlyR). Right, the time course of Ca^{2+} activity changes in VIP INs following uPSEM817 injection (n = 128 cells from four mice). ****P < 0.0001, P = 0.0027, 0.031, 0.19. **d**, Timeline (for **e** and **f**) to examine the acute effects of PSAM^4-GlyR activation on VIP IN activity in the S1 and mechanical paw withdrawal thresholds (von Frey test) in mice 3 days after SNI. **e**, Time course of mechanical thresholds and VIP IN Ca^{2+} activity after a single dose of uPSEM817 (n = 106 cells from five mice). von Frey, P = 0.0008, 0.0007, 0.0031, 0.0079, 0.86, 0.22; Ca^{2+} activity, P = 0.036, 0.024, 0.011, 0.35, 0.59, 0.95. **f**, Correlation between mechanical thresholds and VIP activity for all data points shown in (**e**) (blue line, linear regression; shading, 95% CI; R^2 = 0.98, P < 0.0001). Mean ± SEM. *P < 0.05, **P < 0.01, ***P < 0.001, ****P < 0.0001; *NS*, not significant; by two-sided Wilcoxon test for Ca^{2+} activity (**c, e**) or paired t-test for von Frey (**e**).

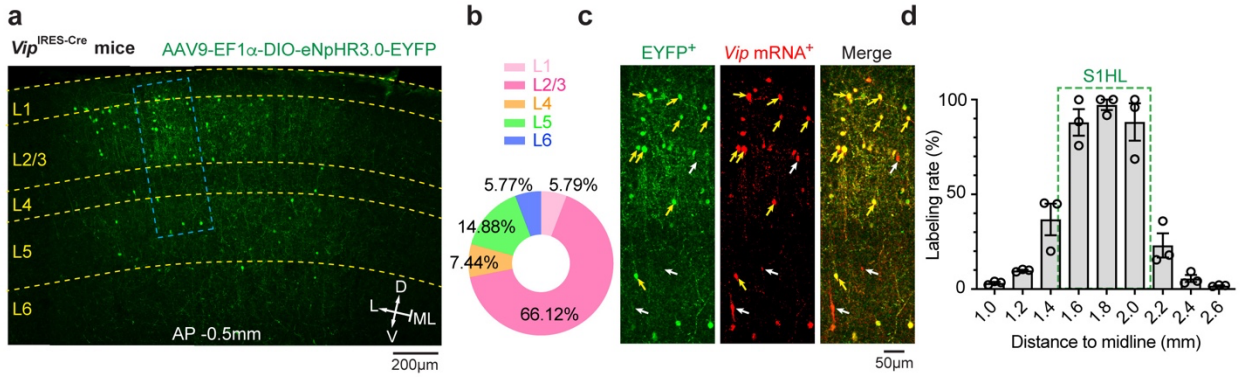

Supplementary Fig. 2 | Validation of halorhodopsin expression in VIP INs in the S1.
a, Fluorescence image of the coronal section showing eNpHR3.0-EYFP expressed mainly in L2/3 of S1 (repeated in 3 mice). **b**, Percentages of EYFP-expressing VIP INs in different layers of S1. **c**, Colocalization of EYFP and *Vip* mRNA-reactive (using fluorescence *in situ* hybridization) somas in the boxed area of (**a**). Yellow and white arrows indicate VIP INs that are positive or negative for EYFP, respectively. **d**, Distribution of labeling rate (mean ± SEM) as a function of distance to midline (n = 3 mice). The labeling rate is defined as the ratio of EYFP$^+$*Vip* mRNA$^+$ to *Vip* mRNA$^+$ cells. S1HL, S1 hindlimb region. L, lateral; ML, midline; D, dorsal; V, ventral.

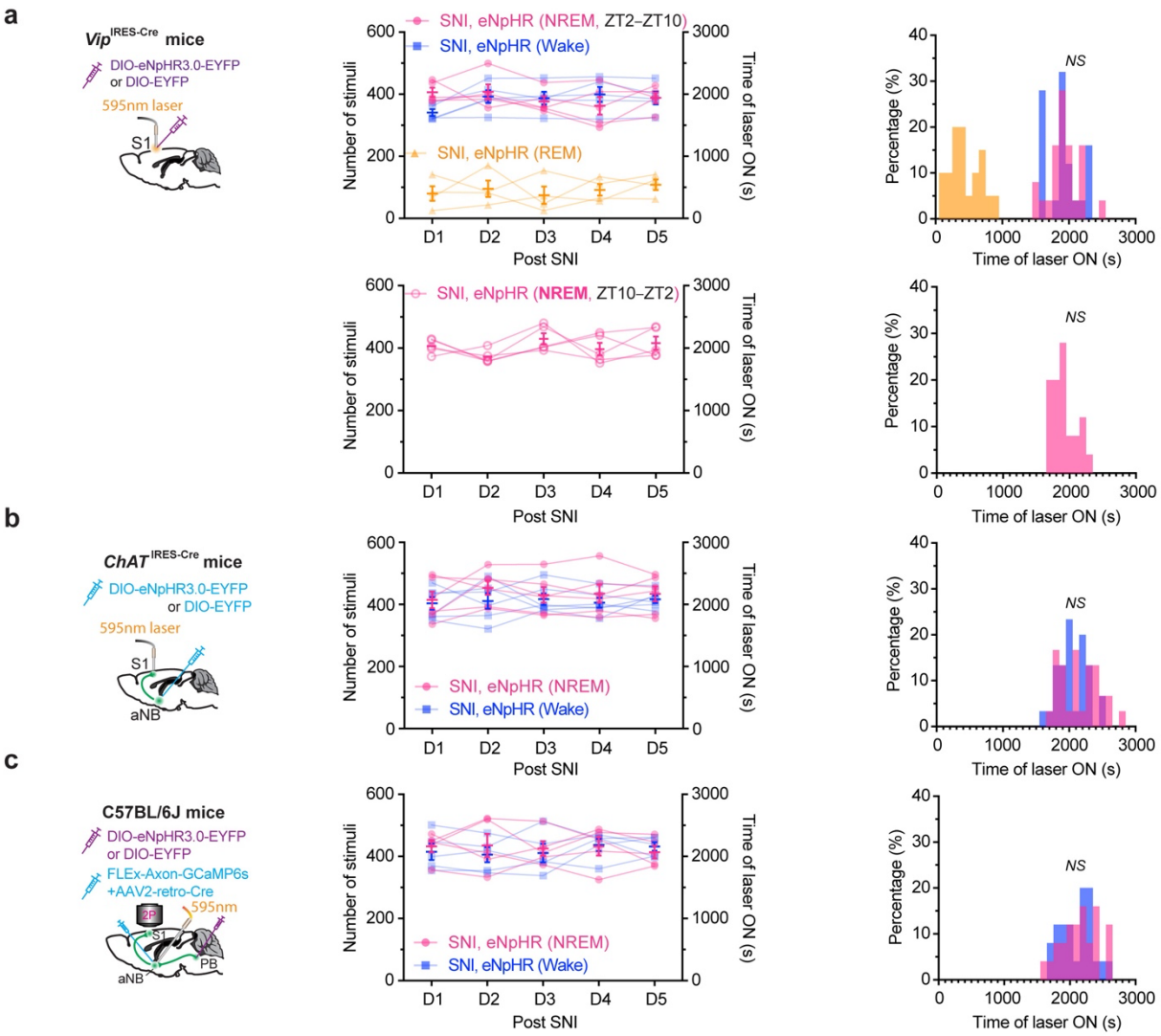

Supplementary Fig. 3 | Laser light delivery data for optogenetic experiments.
a, Light delivery data for optogenetic experiments shown in **Fig. 2f** (n = 5, 5, 4, 5 mice). Left, schematic of experimental design. A 595-nm laser light was delivered each day from ZT2 to ZT10 (see **Methods**), or from ZT10 to ZT2, for 5 consecutive days after SNI. Single stimulus duration, 5 s; frequency, 0.025 Hz for NREM or wake, 0.1 Hz for REM. Middle, number of stimuli (left y-axis) and the total time of laser ON per day (right y-axis) for individual mice from D1–D5 after SNI. Right, distribution of laser ON time for individual mice from D1–D5 for each group. P = 0.70 (ZT2–ZT10; NREM *vs.* Wake). P = 0.47 (NREM; ZT2–ZT10 *vs*. ZT10–ZT2). **b**, Light delivery data for experiments shown in **Fig. 5e** (n = 6 mice per group; P = 0.39). **c**, Light delivery data for experiments shown in **Fig. 6e** (n = 5 mice per group; P = 0.91). Mean ± SEM. *NS*, not significant; by two-sided Kolmogorov-Smirnov test.

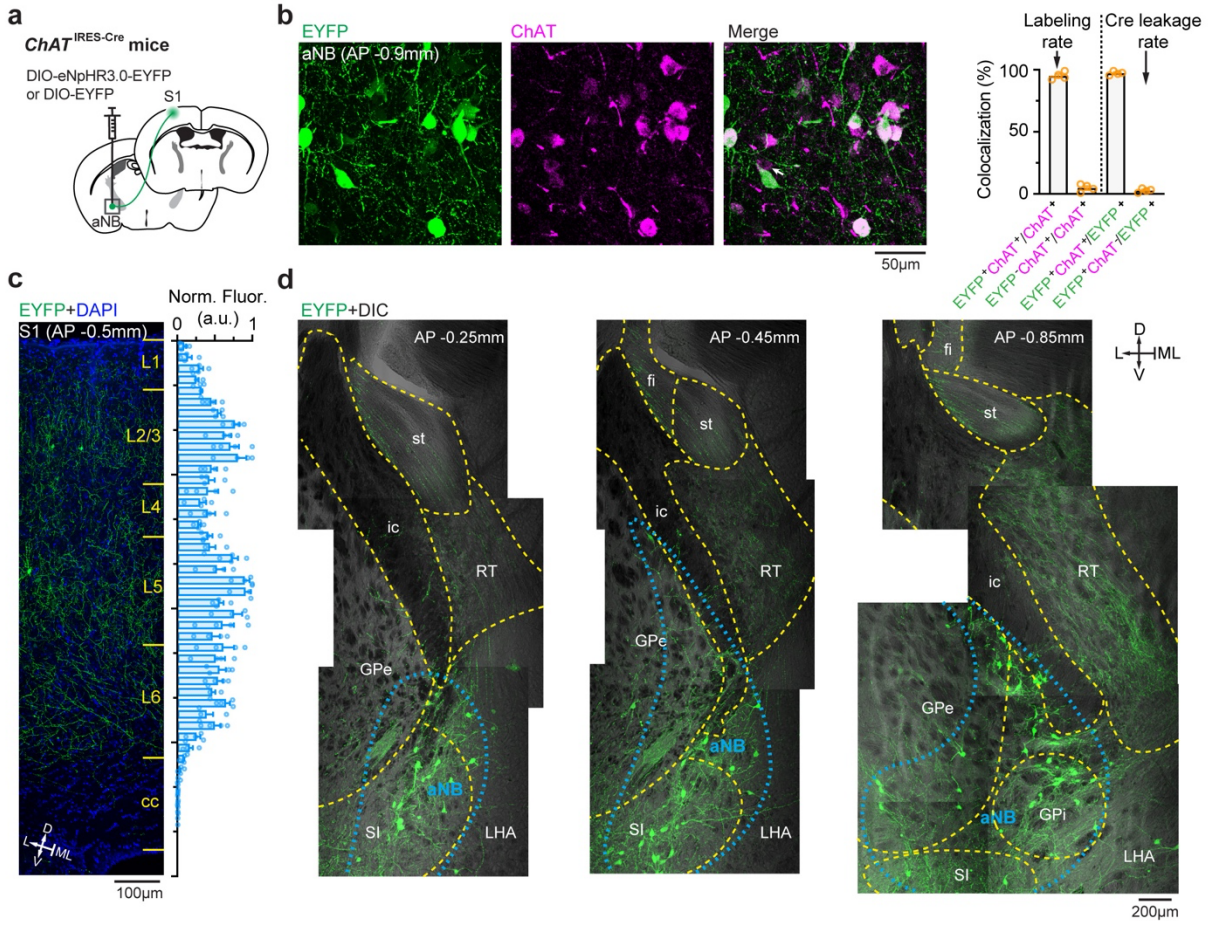

Supplementary Fig. 4 | Basal forebrain cholinergic neurons project to all layers of S1.
a, Schematic of experimental design. AAVs encoding Cre-inducible eNpHR3.0 or EYFP were injected into the aNB of *ChAT*$^{IRES\text{-}Cre}$ mice. **b**, Left, representative fluorescence images of aNB neurons showing the colocalization of EYFP and anti-ChAT immunoreactivity. Right, percentages of colocalized somas in aNB to estimate the cholinergic neuron labeling rate and Cre-leakage rate (mean ± SEM; n = 4 mice). **c**, Fluorescence image (left) and intensity distribution (right; mean ± SEM) of EYFP$^+$ axons across all layers of S1 ipsilateral to the virus injection site (n = 4 mice). a.u., arbitrary units. **d**, Representative fluorescence images at various AP coordinates showing EYFP$^+$ somas in the aNB region of the basal forebrain (the magnocellular region) (4 mice). Blue dashed lines profile the empirical region of NB (the field of magnocellular ChAT$^+$ neurons). L, lateral; ML, midline; D, dorsal; V, ventral; AP, anterior posterior; fi, fimbria; GPe, external globus pallidus; GPi, internal globus pallidus; ic, internal capsule; NB, nucleus basalis; RT, reticular nucleus of the thalamus; S1, primary somatosensory cortex; SI, substantia innominata; st, stria terminalis; LHA, lateral hypothalamic area.

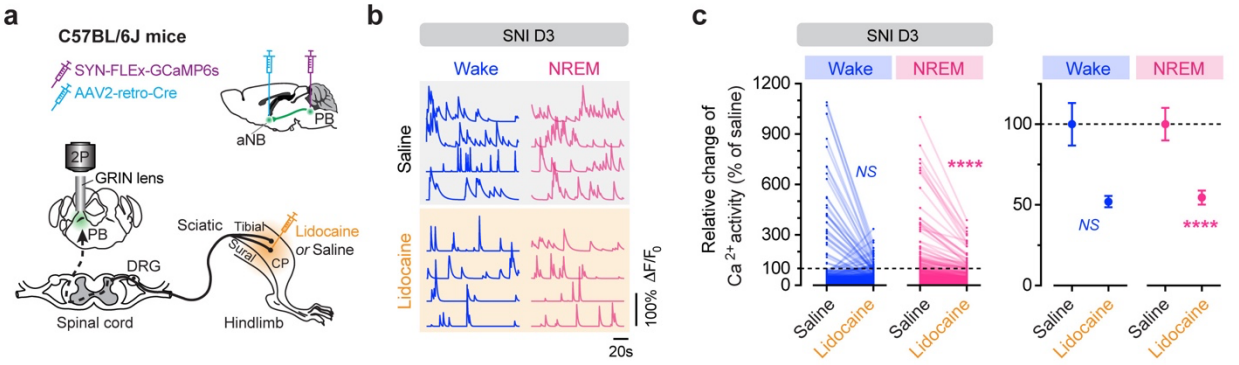

Supplementary Fig. 5 | Local administration of lidocaine at the nerve injury site attenuates PB hyperactivity. **a**, Experimental design. *In vivo* Ca^{2+} imaging was performed in the PB of C57BL/6J mice 3 days after SNI, 0.5 h after saline or lidocaine (a sodium channel blocker) administration at the nerve injury site. **b**, Representative Ca^{2+} traces of PB neurons during wake and NREM sleep after saline or lidocaine administration (3 mice). **c**, Normalized changes of Ca^{2+} activity in PB neurons during wake ($P = 0.85$) and NREM sleep ($P < 0.0001$) after applying saline or lidocaine to peripheral afferents ($n = 222$ cells from three mice). Left, data from individual cells. Right, summary data (mean ± SEM). *NS*, no significant; ****$P < 0.0001$; by Wilcoxon test.